NUMERICAL SIMULATION OF A THERMOACOUSTIC REFRIGERATOR

D. Marx*, **Ph. Blanc-Benon**
Centre acoustique, LMFA, UMR CNRS 5509
Ecole Centrale de Lyon, France
*Email: david.marx@ec-lyon.fr

Abstract

A full Navier-Stokes 2D numerical simulation is made to solve the flow and energy fields in a resonator slice including a 1D stack plate. A stationnary wave is settled in the domain using characteristics method. The temperature difference between the plate ends is compared to linear theory. Some slight differences are found even at low acoustic Mach numbers, which are explained. Some differences at higher Mach number occur due to nonlinearities, and especially temperature nonlinearities.

Introduction

The simulation of a single plate in a thermoacoustic refrigerator is interesting because results may be compared to linear theory. Among quantities of interest is the temperature difference between the ends of the plate. Several studies investigated this temperature difference experimentally or numerically. In some studies agreement were found with linear theory at low Mach numbers [1], [2], and a disagreement appeared at higher Mach numbers due to nonlinear effects. Acoustic Mach number $M_a = u_A/c$ is defined as the ratio of maximum velocity amplitude u_A in the resonator divided by the speed of sound c. It is related to the drive ratio Dr by $M_a = D_r/\gamma$. Disagreement with linear theory occurs when the Mach number exceeds 1%, a low value. This value were found by Worlikar *et al.* in their simulation [2]. This simulation is performed in the vicinity of the plate, so nonlinear effects responsible for the observed disagreement are unlikely to be due to nonlinear wave propagation in the resonator. Another interesting feature is that the agreement between experiments and theory is better near velocity node than near velocity antinode at high Mach numbers [1]. Nevertheless some experiments could not match linear theory predictions, even at low Mach numbers [3], [4].

In the following, a numerical simulation is performed, and temperature difference between the ends of the plate is compared to linear theory. In the choosen configuration, a slight disagreement is found at low Mach numbers, which can be explained. At higher Mach numbers, a bigger disagreement is found, which is due to nonlinear effects. The method which is used to create the standing wave in the domain allows us to get a strong yet linear wave. Hence the nonlinearities do not arise due to nonlinear propagation. Instead they are temperature nonlinearities due to the stack, which were previously observed [5]. In particular it was shown that at high Mach numbers, the temperature oscillation is nonlinear above the plate, whereas the velocity oscillation remains linear. The nonlinear behaviour was found to be stronger near velocity antinodes and for short plates, thus showing that velocity is somehow involved in the process [6].

Methods

The thermoacoustic refrigerator is shown in Fig. 1. The operating frequency $f = \omega/2\pi$ is very high in order to reduce computational time [5]. Hence we take f=20 kHz, corresponding to a wavelength λ =17 mm. The computational domain is referred to as CD. It is

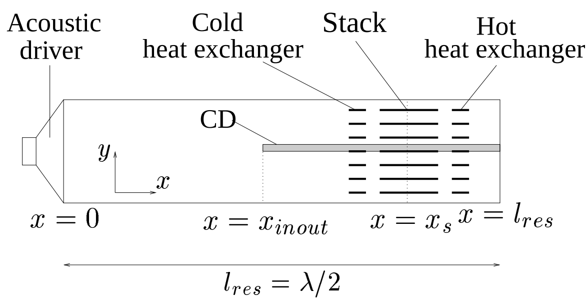

Figure 1: Thermoacoustic refrigerator and computaional domain CD.

located between $x = x_{inout}$ and the resonator end at $x = l_{res} = \lambda/2$. The height of the domain is half the plate spacing, due to stack periodicity. The domain also include a 1D stack plate. An incident propagating wave is injected into the domain through section located at $x = x_{inout}$ using characteristics method [5]. It travels through the domain and is reflected at the resonator end. The reflected wave travels in the direction of the source and leaves the domain at $x = x_{inout}$. The sum of the incident and reflected waves is the standing wave that we need. The total distance the wave travels in the domain being less than a wavelength, there is no time for nonlinear distorsion. Hence the standing wave is linear, even at high Mach numbers. The following equations are solved for the flow:

$$p = \rho r T \tag{1}$$

$$\frac{\partial \rho}{\partial t} + \nabla \cdot (\rho \mathbf{u}) = 0 \quad (2)$$

$$\frac{\partial (\rho \mathbf{u})}{\partial t} + \nabla \cdot (\rho \mathbf{u}\mathbf{u}) + \nabla p = \nabla \cdot \boldsymbol{\tau} \quad (3)$$

$$\frac{\partial T}{\partial t} + \mathbf{u} \cdot \nabla T + (\gamma - 1) T \nabla \cdot \mathbf{u} = \frac{(\gamma-1)}{\rho r} (\Phi + \nabla \cdot (K \nabla T)) \quad (4)$$

T, ρ, and p are respectively the temperature, the density, and the pressure of the fluid. $\mathbf{u}$ is the velocity vector, $\boldsymbol{\tau}$ the stress tensor, and Φ the viscous dissipation. We note K the thermal conductivity of the fluid, r=287 JK^{-1}kg^{-1} the gas constant, γ=1.4 the ratio of specific heats. The 1D equation for the plate temperature T_s is:

$$\rho_s c_s \frac{\partial T_s}{\partial t} = \nabla \cdot (K_s \nabla T_s) + \frac{K}{l} \left(\frac{\partial T}{\partial y} \right)_{plate} \quad (5)$$

ρ_s, c_s and K_s are respectively the density, the specific heat and the thermal conductivity of the plate. l is half the thickness that an equivalent 2D plate would have. The second term on the right hand side of Eq. (5) represents the coupling with the flow. For this coupling we also use the boundary condition $T = T_s$ on the plate surface.

Temperature difference: linear theory

The temperature difference ΔT between the ends of the plate is obtained assuming a zero mean total energy flux along the plate. It is given by:

$$\Delta T = \frac{-L y_0}{4 \rho_m c} P_A^2 \sin(2kx) A_1 \times \left[y_0 K + l K_s - \frac{y_0 c_p}{4 \omega \rho_m c^2 (1 - P_r)} P_A^2 \times (1 - \cos(2kx)) A_2 \right]^{-1} \quad (6)$$

A_1 et A_2 are given by:

$$A_1 = \mathrm{Im} \left[\left(1 - f_\nu^* - \frac{f_\kappa - f_\nu^*}{(1+\epsilon_s)(1+P_r)} \right) \frac{1}{1 - f_\nu^*} \right] \quad (7)$$

$$A_2 = \mathrm{Im} \left[\left(f_\nu^* + \frac{(f_\kappa - f_\nu^*)(1 + \epsilon_s f_\nu / f_\kappa)}{(1+\epsilon_s)(1+P_r)} \right) \frac{1}{(1-f_\nu)(1-f_\nu^*)} \right] \quad (8)$$

We note L the plate length, y_0 half the plate spacing, $k = 2\pi/\lambda$ the wave number, P_r the Prandt number, c_p the isobaric specific heat. $P_A = \rho_m c u_A$ is the maximal pression oscillation amplitude in the resonator. Subscript m indicates mean (time-averaged) quantities. f_ν, f_κ, and ϵ_s are functions which depend on viscous and thermal penetration depths [7]. $*$ denotes the complex conjugate. For expression (6) to be valid, the length L of the plate must be small in comparaison with the wave length λ. Usual assumptions of linear theory are also made [7]. In particular, it is supposed that there is a common mean temperature gradient $dT_m/dx = \Delta T/L$ in the plate and in the fluid, and that this gradient is constant along the plate.

Results

Some simulations are now performed. The fluid is air in normal conditions. For the plate, we take K_s=0.237, ρ_s=900 kgm^3 and c_s=2700 JK^{-1}kg^{-1}. L/λ=0.0088, y_0/δ_κ=1.9 and l/δ_κ=0.41, where $\delta_\kappa = \sqrt{2K/\rho_m c_p \omega}$ is the thermal boundary layer. In the following, two parameters are important: the position x_s of the plate center, which will appear through the non-dimensional number kx_s, and the acoustic Mach number M_a.
In Fig. 2 we plot the temperature difference ΔT as a function of the Mach number, for low Mach numbers. It is compared to linear theory. We observe that even

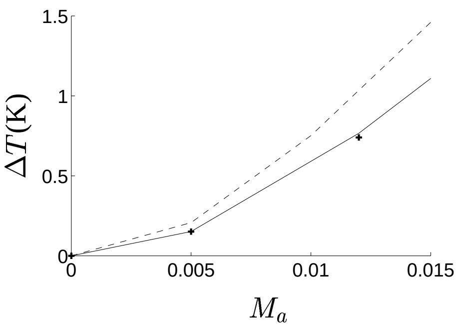

Figure 2: Temperature difference for low Mach numbers as a function of M_a: $+$ calculated, $--$ linear theory (expression 6) —— modified linear theory (expression 9). kx_s=2.35.

for a low value M_a=0.5% (Dr=0.7%) the deviation is about 20%. Two factors can explain this deviation. The first was put forward by Kim *et al.*[4]: the temperature gradient is globally constant along the plate, but not at the extremities of plate. In all configurations tested, this can be responsible for an error of 10%, but not for the errors of 300 % mentionned per Kim *et al.*[4] and Duffourd [3]. Moreover, this factor decreases as the plate length incresases. The second factor is the difference that exists between the mean temperature gradient in the fluid, and the one in the plate. In the linear theory these gradients are assumed to be equal. The mean temperature T_m in the fluid (minus the ambiant temperature T_0) in the section x=cst at the hot extremity of the plate is plotted versus the position y/y_0 in that section. At y=0, the mean temperature is also the temperature of

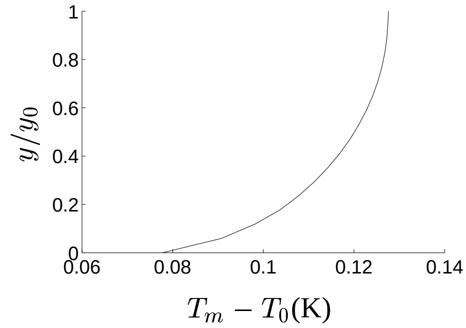

Figure 3: Mean temperature in the section of the channel at the hot extremity of the plate.

the plate. We see that the temperature is not uniform in the section, contrary to linear theory assumptions.
To take account of the two previous factors, the expression (6) is slightly modified as follows:

$$\Delta T = \alpha_1 \frac{-Ly_0}{4\rho_m c} P_A^2 \sin(2kx) A_1 \times \left[\alpha_2 y_0 K + l K_s - \frac{y_0 c_p}{4\omega\rho_m c^2(1-P_r)} P_A^2 \times (1-\cos(2kx))A_2\right]^{-1} \quad (9)$$

α_1 accounts for the non-constant temperature gradient at the extremities of the plate, and α_2 accounts for the difference in mean temperatures in the plate and in the fluid. Two remarks must be done. First α_1 and α_2 are not constants that we choose in order to fit the simulation, they are rigorously computed once the simulation is performed. In particular α_2 is calculated using the spatial average of the mean temperature of the fluid in the hot section of the channel. Second they can be used only as an *a posteriori* correction. If an analytical, *a priori* expression is wanted for both coefficients, an extension of the linear theory valid at the plate ends and giving an expression for the mean temperature in the fluid and in the plate is required (as in Ref. [8]). Data obtained with expression (9) are plotted in Fig. 2. We see that this modified expression fits our numerical results at low Mach numbers.
Now we plot the temperature difference as a function of the Mach number for the whole Mach number range. This is done in Fig. 4 for $kx_s = 2.35$ and in Fig. 5 for $kx_s = 2.9$. For $kx_s = 2.35$, at low Mach numbers, the simulation agrees well with the modified linear theory given by expression (9). A disagreement is found above M_a=1.5%. It is due to nonlinear effects. More precisely, it is mostly due to the nonlinear oscillation of temperature above the plate. Above M_a =1.5%, the temperature deformation indeed increases as the Mach number. As indicated in the introduction, the nonlin-

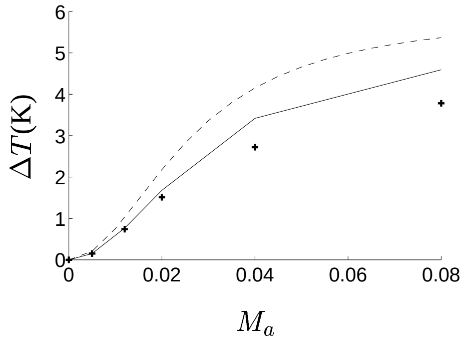

Figure 4: Temperature difference as a function of M_a: $+$ calculated, $--$ linear theory (expression 6) —— modified linear theory (expression 9). kx_s=2.35.

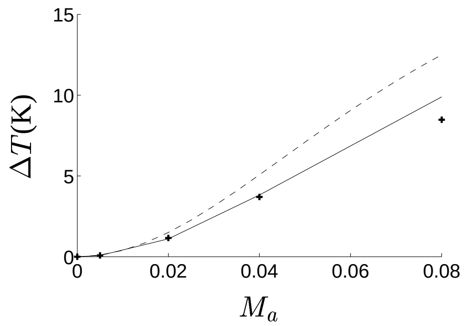

Figure 5: Temperature difference as a function of M_a: $+$ calculated, $--$ linear theory (expression 6) —— modified linear theory (expression 9). kx_s=2.9.

earities of temperature decrease as the plate is pushed toward the velocity antinode. A consequence of that is shown in Fig. 5: for a position kx_s=2.9 closer to the velocity antinode than the previous one, the Mach number at which the temperature difference deviates from linear theory prediction is more than 4%. This value is larger than the value 1.5% found for kx_s=2.35.
We now turn to the effect of the parameter kx_s representing the stack plate position. In Fig. 6 and Fig. 7 we plot the temperature difference ΔT as a function of kx_s for two values of the Mach number: M_a=0.005, and M_a=0.04. For M_a=0.005, we observe that the temperature difference is well predicted by the modified linear theory for all plate positions. In particular, the maximum temperature difference is reached for kx_s=2.35, that is, between the pressure and the velocity antinodes. For a higher value M_a=0.04 of the Mach number, simulations and modified linear theory do not agree for most values of kx_s, as expected at high Mach numbers for which we have nonlinearities. The difference between the calculated curve and the modified linear theory decreases as kx_s increases, which was also found experimentally by Atchley *et al.*[1]. For a value of kx_s high enough, numerical results and modified linear theory

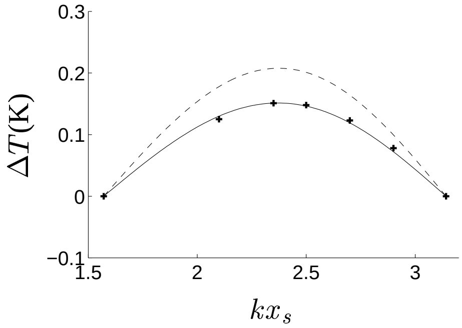

Figure 6: Temperature difference as a function of kx_s: $+$ calculated, $--$ linear theory (expression 6) —— modified linear theory (expression 9). M_a=0.005.

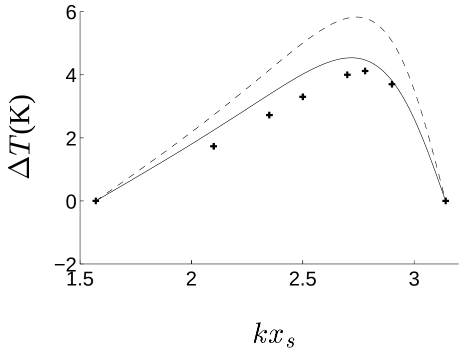

Figure 7: Temperature difference as a function of kx_s: $+$ calculated, $--$ linear theory (expression 6) —— modified linear theory (expression 9). M_a=0.04.

predictions even match. This is the case because nonlinearities in temperature oscillation decrease near the velocity antinode [6]. From Fig. 7 a second observation is made. The optimal value of kx_s for which the temperature difference is maximum is slightly larger than the one predicted by the modified linear theory.

Conclusion

Temperature difference between the extremities of a stack plate were calculated numerically. It was found that even at low Mach numbers, the calculated difference does not always agree with linear theory. Deviations up to 25 % have been observed. Two reasons for these deviations have been found: 1) at the extremities of the plate, the mean temperature is not a linear function of the axial position, 2) the mean temperature in the plate and in the fluid are not equal at the plate ends, contrary to the linear theory assumptions. Taking account of these observations, a slighty modified expression for the temperature difference was given, which agrees with the numerical results at low Mach numbers. The corrections given here are less than 25%, and fail to explain the large deviations (ranging from 200% to 300%) found in some experiments [3][4]. But some parameters may increase the corrrection factor: for example, if the plate thermal conductivity is increased, the second effect will be stronger and the correction factor will be higher.
At high Mach numbers, modified theory and numerical results do not agree, due to nonlinear effects. In particular the deviation is stronger near the velocity antinode. This has been related to the nonlinearity of temperature oscillation, which is itself stronger near velocity antinodes.

Acknowledgments

This work were supported by DGA, computations were performed in part at IDRIS computing center.

References

[1] A. A. Atchley, T. J. Hofler, M. L. Muzerall, M. D. Kite, and C. Ao, ”Acoustically generated temperature gradients in short plates,” J. Acoust. Soc. Am., vol. 88, pp. 251-263,1990.

[2] A. S. Worlikar, and O. Knio, ”Numerical simulation of a thermoacoustic refrigerator. Part 2: Stratified flow around the stack”, J. Comput. Phys., vol. 144, 299-324,1998.

[3] S. Duffourd, ”Réfrigérateur thermoacoustique: études analytiques et expérimentales en vue d’une miniaturisation”, PhD thesis n^{o}2001-06, Ecole Centrale de Lyon, 2001.

[4] Y. T. Kim, S. J. Suh and M. G. Kim, ”Linear resonant duct thermoacoustic refrigerator having regenerator stacks”, in Proccedings of 16th ICA, Seattle, USA, 20-26 June 1998, pp. 821–822.

[5] D. Marx, and Ph. Blanc-Benon, ”Numerical simulation of the coupling between stack and heat exchangers in a thermoacoustic refrigerator”, 9th AIAA-CEAS aeroacoustic conference, Hilton Head, SC, USA, 12-14 May 2003. AIAA Paper 2003-3150.

[6] D. Marx, and Ph. Blanc-Benon, ”Numerical simulation of the stack/heat exchanger coupling in a thermoacoustic refrigerator”, submitted to AIAA Journal.

[7] G. W. Swift, ”Thermoacoustic engines”, J. Acoust. Soc. Am., vol. 84, pp. 1145-1180, 1988.

[8] G. Mozurkewich, ”Time-average distribution in a thermoacoustic stack”, J. Acoust. Soc. Am., vol. 103, pp. 380-388, 1998.